# Cytoprotective effects of transgenic neuroglobin overexpression in an acute and chronic mouse model of ischemic heart disease

# Cytoprotective effects of transgenic neuroglobin overexpression in an acute and chronic mouse model of ischemic heart disease

Evi Luyckx[a*], Bert R. Everaert[b,c*], Bieke Van der Veken[d*], Wendy Van Leuven[a], Jean-Pierre Timmermans[b], Christiaan J. Vrints[c], Guido R. Y. De Meyer[d], Wim Martinet[d], Sylvia Dewilde[a]

[a] Protein chemistry, Proteomics and Epigenetic Signalling, University of Antwerp, Universiteitsplein 1, B-2610 Antwerp, Belgium

[b] Laboratory of Cell Biology and Histology, University of Antwerp, Universiteitsplein 1, B-2610 Antwerp, Belgium

[c] Laboratory of Cellular and Molecular Cardiology, Antwerp University Hospital, Wilrijkstraat 10, B-2650 Edegem, Belgium

[d] Laboratory of Physiopharmacology, University of Antwerp, Universiteitsplein 1, B-2610 Antwerp, Belgium

[*] Co-first authors

**Corresponding author:** Sylvia Dewilde, Protein chemistry, Proteomics and Epigenetic Signalling, University of Antwerp, Universiteitsplein 1 - D.S.426, B-2610 Antwerp, Belgium (sylvia.dewilde@uantwerpen.be, +3232652323)

**Abstract**

Neuroglobin (NGB) is an oxygen-binding protein that is mainly expressed in nervous tissues where it is considered to be neuroprotective during ischemic brain injury. Interestingly, transgenic mice overexpressing NGB reveal cytoprotective effects on tissues lacking endogenous NGB, which might indicate a therapeutic role for NGB in a broad range of ischemic conditions. In the present study, we investigated the effect of NGB overexpression on survival as well as on the size and occurrence of myocardial infarctions (MI) in a mouse model of acute MI (AMI) and a model of advanced atherosclerosis (*ApoE*$^{-/-}$*Fbn1*$^{C1039G+/-}$ mice), in which coronary plaques and MI develop in mice being fed a Western-type diet. Overexpression of NGB significantly enhanced post-AMI survival and reduced MI size by 14 % one week after AMI. Gene expression analysis of the infarction border showed reduction of tissue hypoxia and attenuation of hypoxia-induced inflammatory pathways, which might be responsible for these beneficial effects. In contrast, NGB overexpression did not affect survival or occurrence of MI in the atherosclerotic mice although the incidence of coronary plaques was significantly reduced. In conclusion, NGB proved to act cytoprotectively during MI in the acute setting while this effect was less pronounced in the atherosclerosis model.

**Keywords:** neuroglobin – myocardial infarction – ischemia – atherosclerosis – cytoprotection

## 1. Introduction

Neuroglobin (NGB) is an intracellular oxygen-binding protein related to the globin family [1-3]. It is induced upon neuronal hypoxia and cerebral ischemia and protects against hypoxic and ischemic neuronal injury [4]. The quest for unravelling the functional significance of this evolutionary conserved protein to date has resulted in a variety of hypotheses (for instance enhancing $O_2$ supply to the mitochondria of metabolically active neurons, preventing apoptosis and reducing oxidative stress by scavenging reactive oxygen and nitrogen species) that suggest a neuroprotective effect whose underlying mechanism has not been fully understood yet [5, 6]. In the past few years, the interest to explore the mechanism behind the neuroprotective role of NGB has been expanded to cytoprotection in general, for example after myocardial infarction (MI). Although endogenous NGB expression is restricted to neurons of the central and peripheral nervous systems [7], a transgenic mouse model overexpressing murine NGB under a chicken beta-actin promoter and distal cytomegalovirus enhancer has shown increased NGB expression in multiple cell types and tissues including brain, arteries and heart [8, 9]. According to previous studies, NGB overexpression caused reduction of cerebral infarcts after occlusion of the middle cerebral artery [9, 10] even up to 30 % [9] and in addition, myocardial infarcts produced by occlusion of the left anterior descending (LAD) coronary artery were decreased by approximately 25 % in NGB-overexpressing mice compared to wild type (*WT*) littermates, reflecting the beneficial effect of this globin [9]. The finding that NGB has cytoprotective effects on tissues lacking endogenous NGB expression might indicate a therapeutic role for NGB in a broad range of cardiovascular ischemic conditions such as acute myocardial infarction (AMI) and advanced atherosclerosis.

In the present study, a validated AMI mouse model with permanent ligation of the LAD coronary artery was used to investigate the role of NGB in an acute ischemic setting [11]. Although several therapies, such as administration of anti-platelet drugs and urgent reperfusion of the occluded coronary culprit have proven clinical significance in the setting of AMI, these approaches are still associated with significant mortality and morbidity. In view of the abovementioned observations, the NGB overexpression mouse model driven by its cytoprotective potential [9] is an interesting tool to gain new insights in acute ischemic heart disease. On the other hand, atherosclerotic plaques develop silently over decades and can cause thrombosis or stenotic occlusion, resulting in severe complications, such as MI, stroke or even sudden cardiac death [12]. The *ApoE*$^{-/-}$*Fbn1*$^{C1039G+/-}$ mouse represents a unique model of advanced atherosclerotic plaques with plaque formation even in the coronary arteries, which is almost never the case in *ApoE*$^{-/-}$ mice [13]. The heterozygous mutation *C1039G*$^{+/-}$ in the fibrillin *(Fbn)1* gene causes fragmentation of elastic fibres in the media of the vessel wall [14]. The combination of fragmented elastic fibres with a Western-type diet (WD) in *ApoE*$^{-/-}$*Fbn1*$^{C1039G+/-}$ mice leads to increased plaque formation with important cardiac endpoints

such as MI and sudden death [13]. In the present study, we crossbred the *ApoE*$^{-/-}$*Fbn1*$^{C1039G+/-}$ mouse with a transgenic mouse overexpressing NGB to assess the effect of NGB on the progression of atherosclerosis and its complications. The combined application of a model of AMI and a chronic atherosclerosis model to investigate the role of NGB overexpression, ensures a broad study of the cytoprotective effects of NGB in ischemic heart disease.

## 2. Material and methods

### *2.1 Mice*

#### *2.1.1 AMI model*

Homozygous *(homoz)Ngb-Tg-1* mice (B6.Cg-Tg(CAG-Ngb,-EGFP)1Dgrn/J, stock number 007575, The Jackson Laboratory) were crossbred with C57Bl/6J mice (stock number 000664, Charles River) to produce heterozygous *(hetz)Ngb-Tg-1* mice. By heterozygous breeding, both *hetzNgb-Tg-1* mice and *WT* littermates were obtained. The colony of experimental animals was maintained on a C57BL/6J background for at least 10 generations. All mice used in this experiment were 4 to 5 month old males with a weight of 25 to 30 g.

#### *2.1.2 Atherosclerosis model*

In-house *ApoE*$^{-/-}$*Fbn1*$^{C1039G+/-}$ mice on a C57B6J background were crossbred with *homozNgb-Tg-1* mice (B6.Cg-Tg(CAG-Ngb,-EGFP)1Dgrn/J, stock number 007575, The Jackson Laboratory) to obtain *ApoE*$^{-/-}$*Fbn1*$^{C1039G+/-}$*hetzNgb-Tg-1* mice. Further breeding provided *ApoE*$^{-/-}$*Fbn1*$^{C1039G+/-}$ and *ApoE*$^{-/-}$*Fbn1*$^{C1039G+/-}$*hetzNgb-Tg-1* littermates, which were used in this study. The colony of experimental animals was maintained on a C57BL/6J background for at least 10 generations. All mice used in this experiment were female, and the experiments started at the age of 2 months with a weight of 15 to 20 g and lasted for 4 or 6 months.

For all experiments, mice were housed in a temperature controlled room with a day-night cycle (12/12) and had free access to food and water.

### *2.2 Experimental study design*

#### *2.2.1 AMI model*

AMI was induced by permanent ligation of the LAD coronary artery in *WT* (n=56) and *hetzNgb-Tg-1* (n=21) mice. In brief, mice were anesthetized (Avertin (tribromoethanol) 0.25 mg/g, intraperitoneally), intubated using a 22G intravenous catheter and mechanically ventilated with a small rodent ventilator (MiniVent type 845, Harvard Apparatus, ventilation at 10 µl/g, 180 breaths/min, 2 cm $H_2O$-positive end-expiratory pressure). Body temperature was maintained by using a heating pad. A left parasternal thoracotomy was performed transecting ribs 4 and 5.

After adequate exposure of the heart, the pericardium was cleaved and the LAD was ligated approximately 2 mm below the left atrial appendage using 7-0 polypropylene sutures (Pronova BV-1, Ethicon, Johnson & Johnson). Successful LAD ligation was evidenced by white discoloration of the myocardium, elevation of the ST segment on electrocardiographical monitoring and visual identification of the ligated artery in the infarction zone. Eight *WT* mice were sham-operated, i.e. without ligation of the LAD. Subsequently, the operation wound was closed in layers, mice were weaned from ventilation, extubated and placed under a heat source until full recovery. Mice were monitored until 7 days after AMI and sacrificed.

#### *2.2.2 Atherosclerosis model*

Mice were fed a Western-type diet (WD) (AB Diets) starting at the age of 2 months. Cases of sudden death were documented. At the end of the experiment (17 or 25 weeks of WD) mice were sacrificed.

### *2.3 Plasma cholesterol levels in atherosclerotic mice*

Blood samples were obtained via retro-orbital aspiration and added to 20 µl ethylenediaminetetraacetic acid (EDTA) 10 % to counteract coagulation. Samples were diluted 1:3 with 0.9 % NaCl. Analysis of total plasma cholesterol was performed via the Total Cholesterol Reagent kit (Randox).

### *2.4 Echocardiography*

Transthoracic echocardiograms of *ApoE*$^{-/-}$*Fbn1*$^{C1039G+/-}$ (n=9) and *ApoE*$^{-/-}$*Fbn1*$^{C1039G+/-}$*hetzNgb-Tg-1* mice (n=14) were performed at 17 weeks of WD on anesthetized mice (isoflurane; 3 % for induction and 1.5 % for maintenance, IsoFlo, Abbott) using a Toshiba diagnostic ultrasound system (SSA-700A), equipped with a 15 MHz transducer. End-diastolic diameter (EDD) and end-systolic diameter (ESD) were measured and fractional shortening (FS=[EDD-ESD]/EDD x 100) was calculated.

### *2.5 Survival*

After AMI, survival was studied in *WT* (n=44) and *hetzNgb-Tg-1* (n=20) mice up to 7 days. Long-term survival was studied in *ApoE*$^{-/-}$*Fbn1*$^{C1039G+/-}$ mice (n=15) and *ApoE*$^{-/-}$*Fbn1*$^{C1039G+/-}$*hetzNgb-Tg-1* mice (n=14) up to 17 or 25 weeks of WD.

### *2.6 Histology*

#### *2.6.1 AMI model*

One week after AMI, a cross-sectional segment of the heart of *WT* and *hetzNgb-Tg-1* mice, taken 1 mm below the ligature, was fixed in paraformaldehyde (4 %) and embedded in paraffin (PFPE). PFPE tissues were used for morphometric analysis of infarct size by haematoxylin-eosin (HE) staining. Images were captured with a Zeiss

Axiophot microscope equipped with an Olympus DP70 camera and further processed in Adobe Photoshop to create composite images. Morphometric analysis was performed on composite microscopic images using the Cell$^{P}$ image analysis software. Infarct size was determined on heart cross-sections and computed as percentage of the total left ventricle (LV) ([infarct area/total LV area]x100).

### *2.6.2 Atherosclerosis model*

After sudden death or at the end of the experiment, mice were perfusion-fixed with paraformaldehyde (4 %) via a catheter in the left ventricle for 30 minutes. Subsequently, the proximal ascending aorta, the brachiocephalic artery and the heart of the *ApoE*$^{-/-}$*Fbn1*$^{C1039G+/-}$ and *ApoE*$^{-/-}$*Fbn1*$^{C1039G+/-}$*hetzNgb-Tg-1* mice were dissected. Samples were immediately post fixed in paraformaldehyde (4 %) and PFPE embedded. Serial cross-sections (5 µm) of the aorta and the heart were cut and prepared for histological analysis. Total plaque area was measured on HE stained slides. Sirius red staining was performed to detect collagen. Necrosis was defined as acellular areas filled with necrotic clefts and necrotic debris. Plaque composition was further determined by immunohistochemistry using anti-α-smooth muscle cell actin (F377, Sigma) and anti-Mac 3 (553322, Pharmingen) to detect smooth muscle cells and macrophages, respectively. The occurrence of MI (defined as large fibrotic areas) and coronary plaques was analysed on Masson's trichrome staining (transversal sections). If plaques were present in the coronary arteries, the percentage of stenosis was measured. All images were acquired with Universal Grab 6.1 software using an Olympus BX40 microscope and were quantified with Image J software (NIH).

### *2.7 Gene expression analysis*

Specimens of the infarct border zone, the heart, brain and aorta were harvested, flash-frozen in liquid nitrogen and further processed for total RNA isolation. Following DnaseI (RQ1 RNase-Free DNase, Promega) treatment, RNA concentration and purity were analysed using Nanodrop spectrophotometer (Thermo Scientific) readings at 260 and 280 nm. First-strand cDNA synthesis was performed on 1 µg total RNA with the transcriptor first-strand cDNA synthesis kit (Roche) according to the manufacturer's instructions. For validation of *Ngb* expression levels in heart and aorta, real-time quantitative PCR was performed on a StepOnePlus system (Life Technologies). The parameters for PCR amplification were 95°C for 2 minutes followed by 40 cycles of 95°C for 15 seconds and 60°C for 1 minute. Each real-time PCR reaction comprised Power SYBR Green PCR Master Mix (Applied Biosystems), 10 ng cDNA (RNA equivalents) and 150 nM of each primer: *mPpia* (F-CAGACGCCACTGTCGCTTT, R-TGTCTTTGGAACTTTGTCTGCAA), *mTbp* (F-CCCCACAACTCTTCCATTCT, R-GCAGGAGTGATAGGGGTCAT), *mPgk* (F-CTCCGCTTTCATGTAGAGGAAG, R-GACATCTCCTAGTTTGGACAGTG), *mNgb* (F-

TACAATGGCCGCCAGTTCT, R-TGGTCACTGCAGCATCAATCA). The geNorm algorithm in qBase+ (Version 3.0, BioGazelle) was used to determine the optimal combination of reference genes for internal normalization (i.e. peptidylprolyl isomerase A *(Ppia)*, TATA-box binding protein *(Tbp)* and phosphoglycerate kinase *(Pgk)*). Normalized relative gene expression was determined by the $E^{-\Delta\Delta Cq}$ method. On the other hand, gene expression analysis of hypoxia-induced inflammatory genes at the infarction border zone after AMI was carried out using Taqman gene expression assays (Applied Biosystems) on a LightCycler 480 instrument (Roche). The LightCycler Taqman Master Mix (Roche) was used to obtain transcript levels of hypoxia-inducible factor *(Hif-)1*, intracellular adhesion molecule *(Icam-)1*, vascular cell adhesion molecule *(Vcam-)1*, nitric oxide synthase *(Nos)3* and vascular endothelial growth factor *(Vegf)a* (Applied Biosystems). All qPCR reactions were carried out on 10 ng cDNA (RNA equivalents) as follows: after an initial denaturation-activation step at 95°C for 10 minutes, amplification consisted of 45 cycles of denaturation at 95°C for 10 seconds, annealing at 60°C for 30 seconds and measurement of fluorescence at 72°C for 1 second. The geNorm algorithm was used to determine the optimal combination of reference genes for internal normalization (i.e., hypoxanthine-guanine phosphoribosyltransferase (*Hprt*), translationally controlled tumour protein (*Tpt-)1* and β-2-microglobulin *(B2m)*). Normalized relative gene expression was determined by the $E^{-\Delta\Delta Cq}$ method.

For validation of the mouse model using RT-PCR, amplification of *mNgb* (F-CTCTGGAACATGGCACTGTC, R-ACCACAGCTCCGTAGAGTCG) was performed. The parameters for PCR amplification were as follows: 95°C for 2 minutes followed by 35 cycles of 95°C for 1 minute, 57°C for 1 minute and 72°C for 1 minute, ending with 72°C for 10 minutes. Samples were loaded on a 1 % agarose gel for gel electrophoresis using a GeneRuler 1 kb DNA ladder (Thermo Scientific) as reference.

### *2.8 Statistical analysis*

Data are depicted as mean ± SEM. Statistical analyses were performed with IBM SPSS Statistics 24 and GraphPad Prism 6 software. Statistical tests are specified in each section. $p<0.05$ indicated statistical significance.

## 3. Results

### *3.1 Ngb is overexpressed in heart and aorta after cross-breeding with Ngb-Tg-1 mice*

As a validation of *Ngb* overexpression in *hetz-Ngb-Tg-1* mice, higher *Ngb* expression levels were observed in the brain of *hetzNgb-Tg-1* mice, compared to endogenous *Ngb* expression levels in *WT* mice (Fig. 1a-b). In addition, cross-breeding with the *Ngb-Tg-1* transgenic mouse model significantly induced *Ngb* overexpression in non-

endogenous *Ngb* expressing tissues such as the heart (131 ± 28 fold) (Fig. 1a-c) and aorta (1.85 ± 0.5 fold) (Fig. 1d).

### *3.2 NGB overexpression reduces MI size after AMI*

MI size was 42 % in *WT* versus 28 % in *hetzNgb-Tg-1* mice (Fig. 2a). Microscopic examination of the MI zone in *hetzNgb-Tg-1* mice revealed a distinct infarction pattern as compared to *WT* mice. While *WT* mice mostly displayed complete transmural infarctions, *hetzNgb-Tg-1* overexpressing mice showed a patchier MI area (Fig. 2b).

### *3.3 Survival after AMI is enhanced by NGB overexpression*

The survival rate during the first week after AMI was significantly higher in *hetzNgb-Tg-1* mice (95 % (19/20)) than in *WT* mice (73 % (32/44)) (Fig. 2c), suggesting an important role for NGB in AMI.

### *3.4 NGB overexpression attenuates hypoxia signalling and reduces vascular adhesion molecule expression after AMI*

NGB overexpression has previously been shown to attenuate hypoxia signalling and inflammation in neuronal ischemia [4]. Therefore, transcript levels of hypoxia and inflammation-linked factors were determined in infarct border tissue specimens of *hetzNgb-Tg-1* (n=10) and *WT* mice (n=8) one week after AMI or sham operation of *WT* mice (n=8) (Fig. 2d). AMI-induced upregulation of hypoxia-inducible factor *Hif-1α* (81 % in *WT* vs. 33 % in *hetzNgb-Tg-1* compared to sham), vascular adhesion molecules *Icam-1* (80 % in *WT* vs. -9 % in *hetzNgb-Tg-1* compared to sham) and *Vcam-1* (100 % in *WT* vs. 23 % in *hetzNgb-Tg-1* compared to sham) was significantly attenuated at the mRNA level in *hetzNgb-Tg-1* compared to *WT* mice. *Nos3* and *Vegfa* expression did not significantly differ in the infarct border zone between *hetzNgb-Tg-1* and *WT* mice one week after AMI.

### *3.5 NGB overexpression does not alter plasma cholesterol levels in the atherosclerosis model*

Analysis of total plasma cholesterol revealed no significant difference between both phenotypes after 17 weeks of WD (*ApoE*$^{-/-}$*Fbn1*$^{C1039G+/-}$: 257 ± 64 mg/dl, *ApoE*$^{-/-}$*Fbn1*$^{C1039G+/-}$*hetzNgb-Tg-1*: 151 ± 87 mg/dl) and 25 weeks of WD (*ApoE*$^{-/-}$*Fbn1*$^{C1039G+/-}$: 180 ± 13 mg/dl, *ApoE*$^{-/-}$*Fbn1*$^{C1039G+/-}$*hetzNgb-Tg-1*: 232 ± 38 mg/dl).

### *3.6 The incidence of coronary plaques in atherosclerotic mice is significantly reduced by NGB overexpression*

MI was present in 62 % and 40 % of the *ApoE*$^{-/-}$*Fbn1*$^{C1039G+/-}$ and *ApoE*$^{-/-}$*Fbn1*$^{C1039G+/-}$*hetzNgb-Tg-1* mice respectively, although this reduction was not statistically significant (p=0.22). The location of the infarcts in the heart was random and differed between the septum wall and left or right ventricle in both groups. Concomitant with the presence of MIs, the incidence of coronary plaques was significantly lower in the presence of NGB (*ApoE*$^{-/-}$*Fbn1*$^{C1039G+/-}$: 86 % (19/22), *ApoE*$^{-/-}$*Fbn1*$^{C1039G+/-}$*hetzNgb-Tg-1*: 56 % (10/18)) (Fig. 3a). Coronary stenosis tended

to decrease (74 ± 5 % in *ApoE$^{-/-}$Fbn1$^{C1039G+/-}$* and 52 ± 14 % in *ApoE$^{-/-}$Fbn1$^{C1039G+/-}$hetzNgb-Tg-1*) (p=0.07) (Fig. 3b). Perivascular fibrosis of the coronary arteries was observed in both the presence (44 %) and absence (56 %) of NGB overexpression (Fig. 3c).

### *3.7 NGB overexpression does not affect left ventricular heart function of atherosclerotic mice*

Left ventricular heart function was monitored at 17 weeks of WD. There were no significant differences in either EDD, ESD or FS between *ApoE$^{-/-}$Fbn1$^{C1039G+/-}$* and *ApoE$^{-/-}$Fbn1$^{C1039G+/-}$hetzNgb-Tg-1* mice (Table 1).

### *3.8 Atherosclerotic plaque size and composition do not alter by NGB overexpression*

In the proximal aorta and the brachiocephalic artery, the atherosclerotic plaque size and percentage of necrosis were similar between *ApoE$^{-/-}$Fbn1$^{C1039G+/-}$* and *ApoE$^{-/-}$Fbn1$^{C1039G+/-}$hetzNgb-Tg-1* mice after 17 and 25 weeks of WD (Table 2). Moreover, the amount of collagen and the number of smooth muscle cells and macrophages were not significantly different either, even after 25 weeks of WD (Table 2).

### *3.9 NGB overexpression has no effect on survival of atherosclerotic mice*

No significant difference in survival rate was observed between *ApoE$^{-/-}$Fbn1$^{C1039G+/-}$* mice (60 % (9/15)) and *ApoE$^{-/-}$Fbn1$^{C1039G+/-}$hetzNgb-Tg-1* mice (57 % (8/14)) after 25 weeks of WD (Fig. 3d). Cases of sudden death during the first 10 weeks of WD were unrepresentative and were not taken into account.

## 4. Discussion

Given the strong interplay between globins and oxygen availability in general [15] and NGB upregulation under hypoxic and ischemic conditions in particular [16], the present study aimed to investigate the effect of NGB overexpression in both an acute and a chronic mouse model of myocardial ischemia. To establish high cardiac expression levels of NGB, the constitutive chicken beta-actin promoter and distal CMV enhancer has already been proven to be of great value [17, 18]. Similarly to previous studies reporting on the *Ngb-Tg-1* mouse model, we found induction of significant expression levels of *Ngb* in the brain [8, 10, 19], heart [9] and aorta, giving rise to higher *Ngb* concentrations than observed physiologically. Although endogenous NGB expression does not occur in normal cardiomyocytes, the induction of NGB expression in the heart using a transgenic mouse model led to cytoprotection during acute myocardial ischemia with a significant impact on survival. Indeed, heterozygous overexpression of NGB in *hetzNgb-Tg-1* mice resulted in a lower mortality rate 7 days after induction of AMI, which coincided with a significant reduction in infarction size, and is in line with previous reports [9, 10]. Moreover, while *WT* mice mostly displayed large transmural infarctions one week after AMI, *hetzNgb-Tg-1* mice showed smaller MIs with areas of myocyte survival being most prominent at the epi- and endocardial border.

Interestingly, NGB overexpression led to attenuation of *Hif-1α* transcription in the border zone of the infarcted area. Under hypoxic conditions, the activity of *Hif-1* is upregulated and initiates the transcription of hypoxia-inducible target genes [20, 21]. These gene products in turn restore oxygen homeostasis by inducing glycolysis, erythropoiesis and angiogenesis [22]. The finding that NGB overexpression reduces *Hif-1α* expression during the subacute phase of AMI indicates that NGB overexpression might be able to attenuate hypoxia, hypoxia sensing and/or downstream hypoxia-inducible inflammatory responses. In general, the mechanism of action by which NGB exerts its neuroprotective effects presently remains unclear and is still a topic of debate [23]. Despite the fact that NGB was originally thought to play a role in $O_2$ storage and transport, its weak $O_2$-binding affinity under physiological conditions, in combination with its relatively low endogenous concentrations (± 1 µM) in the brain, could also suggest other functional roles [3, 24, 25]. Even in the transgenic *Ngb-Tg-1* model, where higher *Ngb* transcript levels are present, compared to the physiological range (5 fold in *hetzNgb-Tg-1* brain compared to *WT* brain) [10], it is likely that the weak $O_2$-binding affinity of NGB will prevent NGB from acting as an $O_2$ storage or transport protein. Alternatively, NGB might exert its protective effects by acting as a scavenger of hypoxia-induced reactive oxygen and nitrogen species and thereby reducing oxidative stress [26-28]. On the other hand, the local concentration of NGB might be sufficient to act as a sensor molecule for signal transduction in response to hypoxia. NGB might be triggered by NO, $O_2$, or other signalling molecules to alter its protein conformation and thereby causing associated intracellular signalling which activates cytoprotective pathways [23, 29, 30]. Furthermore, the finding that expression of *Icam-1* and *Vcam-1*, two adhesion molecules that play a role in neutrophil-mediated inflammatory processes [31], was significantly lower in *hetzNgb-Tg-1* mice than in *WT* mice, suggests that NGB overexpression has yet unrecognized anti-inflammatory properties that might be responsible for the beneficial effects on infarction size and cardiac mortality. Given the cytoprotective effects of NGB, administering the protein or boosting its expression levels in the ischemic myocardium may be a promising adjunct in the treatment of myocardial ischemic injury.

Atherosclerotic *ApoE*$^{-/-}$*Fbn1*$^{C1039G+/-}$ mice represent a unique model of advanced atherosclerosis, also in coronary arteries, with human-like complications including MI and sudden death. First, we analysed the effect of NGB on the heart of *ApoE*$^{-/-}$*Fbn1*$^{C1039G+/-}$ mice in this model of chronic myocardial ischemia. Although the decreased incidence of MIs in *ApoE*$^{-/-}$*Fbn1*$^{C1039G+/-}$*hetzNgb-Tg-1* mice did not reach statistical significance, the incidence of coronary plaques was significantly reduced by 31 % in NGB positive mice, indicating the cytoprotective effect of NGB as shown in the AMI model. However, NGB did not affect cardiac function as shown by echocardiography. Second, analysis of plaque progression in the proximal aorta and brachiocephalic artery showed that NGB

overexpression had no effect on plaque size or composition between *ApoE*$^{-/-}$*Fbn1*$^{C1039G+/-}$ and *ApoE*$^{-/-}$*Fbn1*$^{C1039G+/-}$*hetzNgb-Tg-1* mice. These findings contrast with the results of previous studies showing decreased neointima formation and plaque inflammation after targeting hypoxia via the reduction of *Hif-1α* [32, 33]. It has been demonstrated that NGB acts protectively under hypoxic and ischemic conditions both *in vitro* and *in vivo* [4, 9, 28, 34, 35]. It is important to note that very pronounced hypoxic or ischemic conditions (e.g. hypoxic chambers, surgical occlusion such as the AMI procedure carried out in the present study) were used in most of these studies. In atherosclerosis, the level of hypoxia is milder and probably does not reach the threshold of severity needed to fully benefit from NGB overexpression.

In conclusion, NGB acts cytoprotectively during MI in an acute setting (ligation of the LAD coronary artery), but this effect is less pronounced in a chronic setting (MI after stenosis of coronary arteries). Overexpression of NGB significantly enhanced post-AMI survival and reduced MI size one week after AMI. These beneficial effects in the setting of AMI might be explained by reduction of tissue hypoxia and attenuation of hypoxia-induced inflammatory pathways. Although the incidence of coronary plaques was significantly reduced by NGB overexpression in a coronary atherosclerosis model, this did not translate into a long term functional or survival benefit.

## 5. Conflict of interest

The authors declare that they have no conflict of interest.


## 6. Acknowledgements

The authors would like to thank Rita Van den Bossche, Anne Boerekamps, Nadine de Nijs, Debby Van Dam, Inge Bats and Sanne Lauryssen for equipment and technical support.

## 7. Compliance with ethical standards


### Sources of funding

This work was supported by the University of Antwerp. Evi Luyckx is a fellow of the Fund for Scientific Research (FWO)-Flanders, Bieke Van der Veken's PhD scholarship was granted by the University of Antwerp (DOCPRO-BOF) and Wendy Van Leuven was a fellow of the Agency for Innovation by Science and Technology (IWT).


### Research involving animals

All animal procedures were performed in compliance with the guidelines from Directive 2010/63/EU of the European Parliament on the protection of animals used for scientific purposes and approved by the Ethics committee of the University of Antwerp.

**8. References**


1. Geuens E, Brouns I, Flamez D, Dewilde S, Timmermans J-P, Moens L (2003) A Globin in the Nucleus! J Biol Chem 278: 30417-30420.

2. Dewilde S, Kiger L, Burmester T, Hankeln T, Baudin-Creuza V, Aerts T, Marden MC, Caubergs R, Moens L (2001) Biochemical Characterization and Ligand Binding Properties of Neuroglobin, a Novel Member of the Globin Family. J Biol Chem 276: 38949-38955.

3. Burmester T, Weich B, Reinhardt S, Hankeln T (2000) A vertebrate globin expressed in the brain. Nature 407: 520-523.

4. Sun Y, Jin K, Mao XO, Zhu Y, Greenberg DA (2001) Neuroglobin is up-regulated by and protects neurons from hypoxic-ischemic injury. Proc Natl Acad Sci U S A 98: 15306-15311.

5. Burmester T, Hankeln T (2009) What is the function of neuroglobin? J Exp Biol 212: 1423-1428.

6. Hankeln T, Ebner B, Fuchs C, Gerlach F, Haberkamp M, Laufs TL, Roesner A, Schmidt M, Weich B, Wystub S, Saaler-Reinhardt S, Reuss S, Bolognesi M, Sanctis DD, Marden MC, Kiger L, Moens L, Dewilde S, Nevo E, Avivi A, Weber RE, Fago A, Burmester T (2005) Neuroglobin and cytoglobin in search of their role in the vertebrate globin family. J Inorg Biochem 99: 110-119.

7. Reuss S, Saaler-Reinhardt S, Weich B, Wystub S, Reuss MH, Burmester T, Hankeln T (2002) Expression analysis of neuroglobin mRNA in rodent tissues. Neuroscience 115: 645-656.

8. Khan AA, Sun Y, Jin K, Mao XO, Chen S, Ellerby LM, Greenberg DA (2007) A neuroglobin-overexpressing transgenic mouse. Gene 398: 172-176.

9. Khan AA, Wang Y, Sun Y, Mao XO, Xie L, Miles E, Graboski J, Chen S, Ellerby LM, Jin K, Greenberg DA (2006) Neuroglobin-overexpressing transgenic mice are resistant to cerebral and myocardial ischemia. Proc Natl Acad Sci U S A 103: 17944-17948.

10. Raida Z, Hundahl CA, Nyengaard JR, Hay-Schmidt A (2013) Neuroglobin Over Expressing Mice: Expression Pattern and Effect on Brain Ischemic Infarct Size. PLoS One 8: e76565.

11. Lutgens E, Daemen MJAP, de Muinck ED, Debets J, Leenders P, Smits JFM (1999) Chronic myocardial infarction in the mouse: cardiac structural and functional change. Cardiovasc Res 41: 586-593.

12. Libby P (2013) Mechanisms of Acute Coronary Syndromes and Their Implications for Therapy. N Engl J Med 368: 2004-2013.

13. Van der Donckt C, Van Herck JL, Schrijvers DM, Vanhoutte G, Verhoye M, Blockx I, Van Der Linden A, Bauters D, Lijnen HR, Sluimer JC, Roth L, Van Hove CE, Fransen P, Knaapen MW, Hervent A-S, De Keulenaer GW, Bult H, Martinet W, Herman AG, De Meyer GRY (2015) Elastin fragmentation in atherosclerotic mice leads to intraplaque neovascularization, plaque rupture, myocardial infarction, stroke, and sudden death. Eur Heart J 36: 1049-1058.

14. Van Herck JL, De Meyer GRY, Martinet W, Van Hove CE, Foubert K, Theunis MH, Apers S, Bult H, Vrints CJ, Herman AG (2009) Impaired Fibrillin-1 Function Promotes Features of Plaque Instability in Apolipoprotein E–Deficient Mice. Circulation 120: 2478-2487.

15. Burmester T, Hankeln T (2014) Function and evolution of vertebrate globins. Acta Physiologica 211: 501-514.

16. Haines B, Demaria M, Mao X, Xie L, Campisi J, Jin K, Greenberg DA (2012) Hypoxia-inducible factor-1 and neuroglobin expression. Neurosci Lett 514: 137-140.

17. Kimura W, Xiao F, Canseco DC, Muralidhar S, Thet S, Zhang HM, Abderrahman Y, Chen R, Garcia JA, Shelton JM, Richardson JA, Ashour AM, Asaithamby A, Liang H, Xing C, Lu Z, Zhang CC, Sadek HA (2015) Hypoxia fate mapping identifies cycling cardiomyocytes in the adult heart. Nature 523: 226-230.

18. Raulf A, Horder H, Tarnawski L, Geisen C, Ottersbach A, Röll W, Jovinge S, Fleischmann BK, Hesse M (2015) Transgenic systems for unequivocal identification of cardiac myocyte nuclei and analysis of cardiomyocyte cell cycle status. Basic Res Cardiol 110: 33.

19. Taylor JM, Kelley B, Gregory EJ, Berman NEJ (2014) Neuroglobin Overexpression Improves Sensorimotor Outcomes in a Mouse Model of Traumatic Brain Injury. Neurosci Lett 0: 125-129.

20. Albrecht M, Zitta K, Bein B, Wennemuth G, Broch O, Renner J, Schuett T, Lauer F, Maahs D, Hummitzsch L, Cremer J, Zacharowski K, Meybohm P (2012) Remote ischemic preconditioning regulates HIF-1α levels, apoptosis and inflammation in heart tissue of cardiosurgical patients: a pilot experimental study. Basic Res Cardiol 108: 314-326.

21. Zhao H-X, Wang X-L, Wang Y-H, Wu Y, Li X-Y, Lv X-P, Zhao Z-Q, Zhao R-R, Liu H-R (2009) Attenuation of myocardial injury by postconditioning: role of hypoxia inducible factor-1α. Basic Res Cardiol 105: 109-118.

22. Cadenas S, Aragonés J, Landázuri MO (2010) Mitochondrial reprogramming through cardiac oxygen sensors in ischaemic heart disease. Cardiovasc Res 88: 219-228.

23. Ascenzi P, di Masi A, Leboffe L, Fiocchetti M, Nuzzo MT, Brunori M, Marino M (2016) Neuroglobin: From structure to function in health and disease. Mol Aspects Med 52: 1-48.

24. Fago A, Hundahl C, Dewilde S, Gilany K, Moens L, Weber RE (2004) Allosteric Regulation and Temperature Dependence of Oxygen Binding in Human Neuroglobin and Cytoglobin: Molecular mechanisms and physiological significance. J Biol Chem 279: 44417-44426.

25. Kiger L, Uzan J, Dewilde S, Burmester T, Hankeln T, Moens L, Hamdane D, Baudin-Creuza V, Marden MC (2004) Neuroglobin Ligand Binding Kinetics. IUBMB Life 56: 709-719.

26. Fordel E, Thijs L, Moens L, Dewilde S (2007) Neuroglobin and cytoglobin expression in mice. FEBS Journal 274: 1312-1317.

27. Herold S, Fago A, Weber RE, Dewilde S, Moens L (2004) Reactivity Studies of the Fe(III) and Fe(II)NO Forms of Human Neuroglobin Reveal a Potential Role against Oxidative Stress. J Biol Chem 279: 22841-22847.

28. Liu J, Yu Z, Guo S, Lee S-R, Xing C, Zhang C, Gao Y, Nichools DG, Lo EH, Wang X (2009) Effects of neuroglobin over-expression on mitochondrial function and oxidative stress following hypoxia/reoxygenation in cultured neurons. J Neurosci Res 87: 164-170.

29. Watanabe S, Takahashi N, Uchida H, Wakasugi K (2012) Human Neuroglobin Functions as an Oxidative Stress-responsive Sensor for Neuroprotection. J Biol Chem 287: 30128-30138.

30. Petersen MG, Dewilde S, Fago A (2008) Reactions of ferrous neuroglobin and cytoglobin with nitrite under anaerobic conditions. J Inorg Biochem 102: 1777-1782.

31. Kukielka GL, Hawkins HK, Michael L, Manning AM, Youker K, Lane C, Entman ML, Smith CW, Anderson DC (1993) Regulation of intercellular adhesion molecule-1 (ICAM-1) in ischemic and reperfused canine myocardium. J Clin Invest 92: 1504-1516.

32. Christoph M, Ibrahim K, Hesse K, Augstein A, Schmeisser A, Braun-Dullaeus RC, Simonis G, Wunderlich C, Quick S, Strasser RH, Poitz DM (2014) Local inhibition of hypoxia-inducible factor reduces neointima formation after arterial injury in ApoE−/− mice. Atherosclerosis 233: 641-647.

33. Tsai S-H, Huang P-H, Hsu Y-J, Peng Y-J, Lee C-H, Wang J-C, Chen J-W, Lin S-J (2016) Inhibition of hypoxia inducible factor-1α attenuates abdominal aortic aneurysm progression through the down-regulation of matrix metalloproteinases. Sci Rep 6: 28612-28622.

34. Li RC, Guo SZ, Lee SK, Gozal D (2010) Neuroglobin Protects Neurons against Oxidative Stress in Global Ischemia. J Cereb Blood Flow Metab 30: 1874-1882.

35. Shao G, Gong KR, Li J, Xu XJ, Gao CY, Zeng XZ, Lu GW, Huo X (2009) Antihypoxic Effects of Neuroglobin in Hypoxia-Preconditioned Mice and SH-SY5Y Cells. Neurosignals 17: 196-202.

## 9. Tables

**Table 1.** Assessment of the left ventricular function of *ApoE$^{-/-}$Fbn1$^{C1039G+/-}$* versus *ApoE$^{-/-}$Fbn1$^{C1039G+/-}$hetzNgb-Tg-1* mice after 17 weeks of WD.

| | ***ApoE$^{-/-}$Fbn1$^{C1039G+/-}$*** | ***ApoE$^{-/-}$Fbn1$^{C1039G+/-}$hetzNgb-Tg-1*** |
|---|---|---|
| **EDD (mm)** | 3.4 ± 0.2 | 3.7 ± 0.2 |
| **ESD (mm)** | 2.2 ± 0.2 | 2.3 ± 0.2 |
| **FS (%)** | 36 ± 2 | 38 ± 2 |

*ApoE$^{-/-}$Fbn1$^{C1039G+/-}$* (n=9) and *ApoE$^{-/-}$Fbn1$^{C1039G+/-}$hetzNgb-Tg-1* (n=14) mice. Independent samples t-test showed no significance ($p>0.05$).

**Table 2.** Plaque characteristics of the proximal ascending aorta and brachiocephalic artery from *ApoE$^{-/-}$ Fbn1$^{C1039G+/-}$* and *ApoE$^{-/-}$Fbn1$^{C1039G+/-}$hetzNgb-Tg-1* mice at 17 and 25 weeks of WD.

| | ***ApoE$^{-/-}$Fbn1$^{C1039G+/-}$*** | ***ApoE$^{-/-}$Fbn1$^{C1039G+/-}$ hetzNgb-Tg-1*** | ***ApoE$^{-/-}$Fbn1$^{C1039G+/-}$*** | ***ApoE$^{-/-}$Fbn1$^{C1039G+/-}$ hetzNgb-Tg-1*** |
|---|---|---|---|---|
| | **17 weeks of WD** | | **25 weeks of WD** | |
| *Proximal ascending aorta* | | | | |
| **Plaque size (.10$^4$ µm$^2$)** | 60.0 ± 6.3 | 59.3 ± 6.9 | 73.8 ± 9.1 | 86.3 ± 20.9 |
| **Necrotic core (%)** | 11.9 ± 2.5 | 10.2 ± 2.3 | 8.7 ± 1.8 | 11.2 ± 1.5 |
| **Collagen (%)** | 10.3 ± 1.2 | 11.7 ± 1.6 | 16.2 ± 0.9 | 14.0 ± 1.4 |
| **Smooth muscle cells (%)** | 6.3 ± 0.6 | 7.1 ± 0.8 | 14.1 ± 1.4 | 12.9 ± 1.2 |
| **Macrophages (%)** | 0.8 ± 0.1 | 1.0 ± 0.2 | 4.0 ± 0.5 | 3.9 ± 1.0 |
| *Brachiocephalic artery* | | | | |
| **Plaque size (.10$^4$ µm$^2$)** | 33.6 ± 2.9 | 33.0 ± 4.0 | 35.6 ± 5.1 | 43.6 ± 4.8 |
| **Necrotic core (%)** | 9.5 ± 2.1 | 12.5 ± 2.2 | 8.7 ± 1.8 | 11.2 ± 1.5 |
| **Collagen (%)** | 9.5 ± 1.6 | 12.6 ± 1.6 | 22.1 ± 3.2 | 25.7 ± 2.3 |
| **Smooth muscle cells (%)** | 6.9 ± 1.1 | 5.3 ± 1.0 | 2.5 ± 0.3 | 3.2 ± 0.3 |
| **Macrophages (%)** | 0.5 ± 0.1 | 0.6 ± 0.1 | 2.6 ± 0.4 | 2.4 ± 0.5 |

Sample size n=8-10. Independent samples t-test showed no significance ($p>0.05$).

**10. Figures**

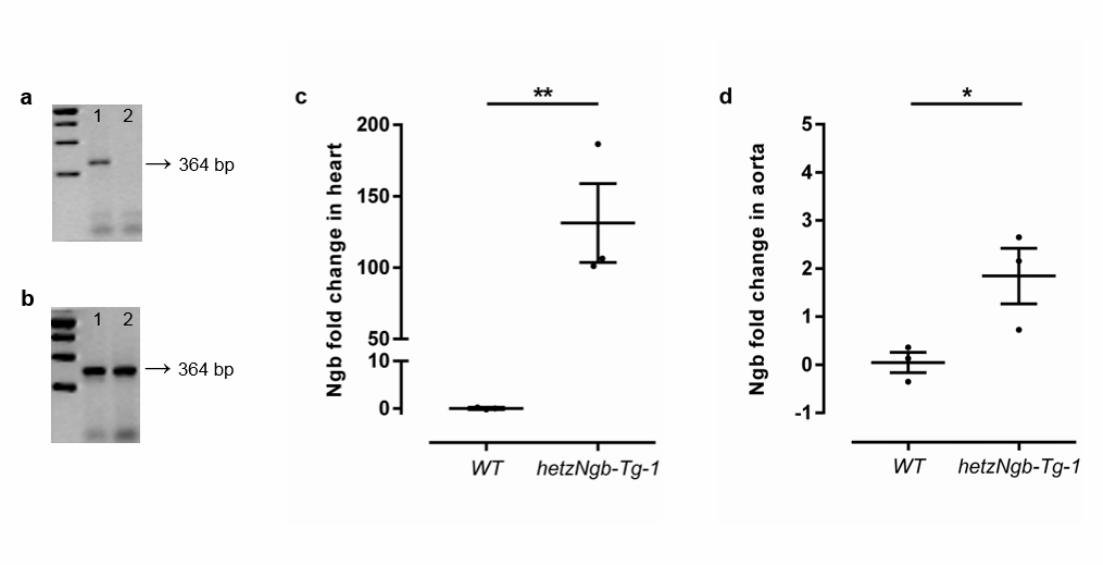


**Fig. 1 Validation of the *hetzNgb-Tg-1* mouse model at the transcript level** a-b) Agarose (1 %) gel electrophoresis of RT-PCR amplicons from 1: brain and 2: heart tissue of an a) *WT* and b) *hetzNgb-Tg-1* mouse with a GeneRuler 1 kb DNA ladder as reference; c) Relative expression levels of *Ngb* in the heart expressed as fold changes in *hetzNgb-Tg-1* mice (n=3) compared to *WT* mice (n=3). ** $p < 0.01$ Independent samples t-test; d) Relative expression levels of *Ngb* in the aorta expressed as fold changes in *hetzNgb-Tg-1* mice (n=3) compared to *WT* mice (n=3). * $p < 0.05$ Independent samples t-test;

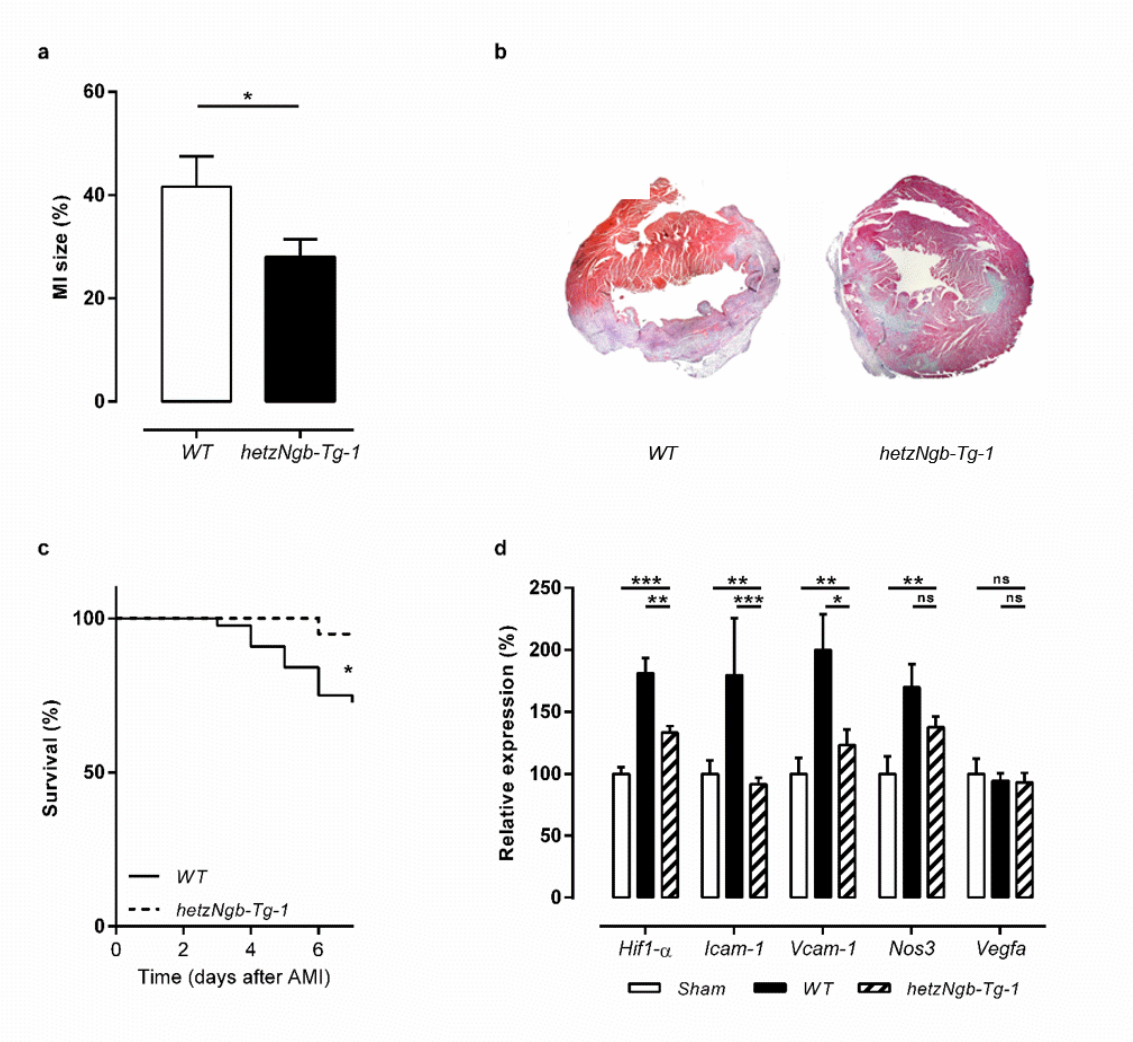


**Fig. 2 Analysis of the AMI model: MI size, survival and gene expression of hypoxia-induced inflammatory genes at the infarction border zone** a) Infarct size in *WT* (n=10) versus *hetzNgb-Tg-1* (n=14) mice after AMI. *p<0.05 (independent samples t-test); b) Representative images of a transmural infarction of a *WT* mouse (left) versus a patchy infarction in an *hetzNgb-Tg-1* mouse (right) 7 days after AMI; c) Kaplan-Meier plot of survival up to 7 days after AMI in *WT* (n=44) and *hetzNgb-Tg-1* (n=20) mice. Kaplan-Meier analysis: *p<0.05. Mortality during surgical procedures was not taken into account; d) Relative expression levels of *Hif-1α*, *Icam-1*, *Vcam-1*, *Nos3* and *Vegfa* in the infarction border zone of *WT* (n=8), *hetzNgb-Tg-1* (n=10) and sham-operated *WT* (n=8) mice. *p<0.05, **p<0.01, ***p<0.001, ns: not significant (Kruskal-Wallis and Mann-Whitney tests).

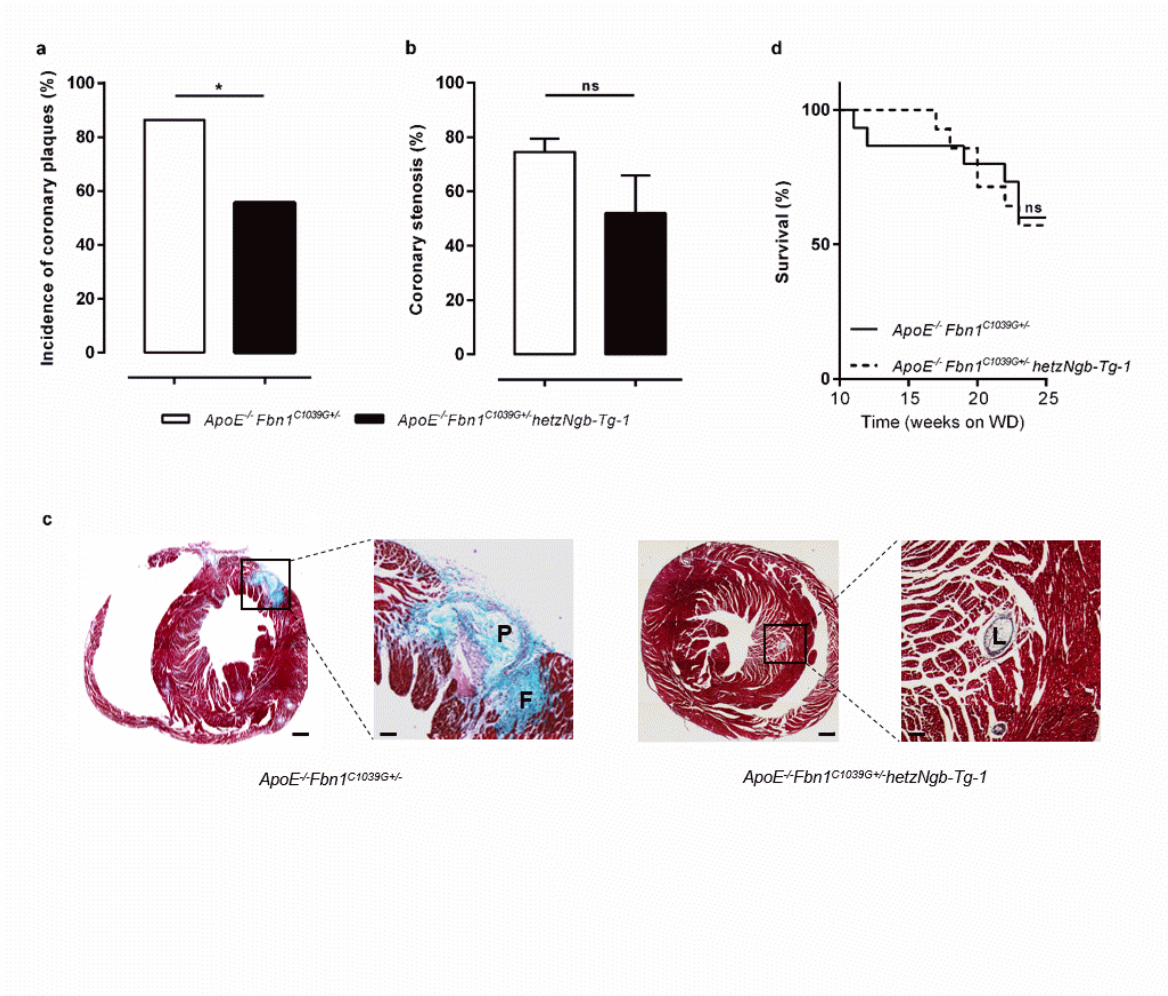


**Fig. 3 Analysis of the atherosclerosis model: coronary characteristics and survival** a) Incidence of coronary plaques in a group of *ApoE*$^{-/-}$*Fbn1*$^{C1039G+/-}$ (n=22) versus *ApoE*$^{-/-}$*Fbn1*$^{C1039G+/-}$*hetzNgb-Tg-1* (n=18) mice. *p<0.05 (Fisher's exact test); b) Coronary stenosis (%) in *ApoE*$^{-/-}$*Fbn1*$^{C1039G+/-}$ (n=14) and *ApoE*$^{-/-}$*Fbn1*$^{C1039G+/-}$*hetzNgb-Tg-1* (n=7) mice. Independent samples t-test showed no significance (ns); c) Masson's trichrome staining of the heart and magnification of the boxed area revealed the presence of coronary plaques and fibrosis of heart tissue. (scale bar left part = 300µm, scale bar magnification = 50µm); L=lumen, P=plaque, F=fibrosis; Representative images were selected from 8-10 evaluated samples; d) Kaplan-Meier plot of survival up to 25 weeks of WD in *ApoE*$^{-/-}$*Fbn1*$^{C1039G+/-}$ (n=15) and *ApoE*$^{-/-}$*Fbn1*$^{C1039G+/-}$*hetzNgb-Tg-1* (n=14) mice. Mortality in the first 10 weeks of WD was not taken into account. Kaplan-Meier analysis: not significant (ns).